

ORIGINAL PAPER



The sphenothmoidal sinus and the modified anatomy of the related structures

MUGUREL CONSTANTIN RUSU¹⁾, SORIN HOSTIUC²⁾, ANDREI GHEORGHE MARIUS MOTOC³⁾,
CARMEN AURELIA MOGOANTĂ⁴⁾, JULIETTA CRISTINA SAVA³⁾, MIHAI SĂNDULESCU⁵⁾

¹⁾Division of Anatomy, Department 1, Faculty of Dental Medicine, Carol Davila University of Medicine and Pharmacy, Bucharest, Romania

²⁾Division of Legal Medicine and Bioethics, Faculty of Dental Medicine, Carol Davila University of Medicine and Pharmacy, Bucharest, Romania

³⁾Division of Anatomy and Embryology, Faculty of Medicine, Victor Babeş University of Medicine and Pharmacy, Timișoara, Romania

⁴⁾Department of ENT, University of Medicine and Pharmacy of Craiova, Romania

⁵⁾Division of Implant Prosthetic Rehabilitation, Faculty of Dental Medicine, Carol Davila University of Medicine and Pharmacy, Bucharest, Romania

Abstract

The anterior extent of the sphenoidal sinus in the posterior ethmoid was less investigated. Our purpose was to study whether, or not, the occurrence of a sphenothmoidal sinus (SES) relates to a sagittally-shortened ethmoid. A retrospective cone-beam computed tomography (CBCT) was performed on 36 patient files. In six patients were found SES extended anteriorly above the posterior third of the middle turbinate (MT). Two of these patients had bilateral SES with ethmoidal chambers included in the lateral and superior nasal walls and draining in the sphenothmoidal recesses. The correlation between the *nasion-to-concha sphenoidalis* distance and the presence of SES was statistically significant (less than 40 mm in SES cases and more than 40 mm in non-SES cases). We also found: (i) superior turbinates (STs) with ethmoidal and sphenoidal insertions on one side and ethmoidal and maxillary insertions on the opposite side (the maxillary insertion of ST modifies surgical landmarks and was not previously reported), (ii) MT perforation and (iii) pterygoid recess of the maxillary sinus located beneath the pterygopalatine ganglion fossa. The SES thus shortens sagittally the lateral nasal wall but does not modify its morphology. The MT perforation, ST maxillary insertion and the pterygoid recess are rare anatomic variants not reported previously in our knowledge.

Keywords: ethmoid cells, sphenoidal sinus, nasal turbinate, anatomic variation, maxillary sinus.

Introduction

The ethmoid derives from the cartilaginous nasal capsule, being different from all the other sinuses which extend from the ethmoid into membranous bone [1]. In the 3rd fetal month, the primitive sphenoidal (sphenoid) sinus (SS) appears as the evagination of nasal mucosa into the cartilaginous nasal capsule (primary pneumatization) [2]. That pouch-like chondral cavity is termed sphenoid turbinate or *ossiculum Bertini* [2]. Further, in the 4th month, the evagination penetrates the sphenoid bone (secondary pneumatization) [3]. In other words, during a neosinus pneumatization, it “moves” from an ethmoidal anatomical site to a different one, without remnants in the first location. The full complement of ethmoidal cells is present in the newborn and the SS is completed after the age of 7–8 [3, 4].

SS has a considerable degree of anatomic variability [5, 6], which is equally inter- and intra-subject [7]. The sagittal pneumatization of the SS was classified in four types: conchal (fetal), pre-sellar, sellar and post-sellar [7, 8] (if the post-sellar type is omitted, only three types [3] will result) that relate the sinus to the *sella turcica* but do not indicate to what extent the SS invades the normal anatomic situs of the ethmoid labyrinth. Agenesis of SS

was regarded as a supplemental type of sagittal pneumatization [9]. These sella-related patterns do not take into account the sagittal position of the ethmoidal spine (process) and the inconstant *alae minimae* of Luschka that project anteriorly from the *jugum sphenoidale* towards the ethmoidal sieve-plate (*lamina cribriformis*) [10] and thus could reach a coronal plane anterior to the tails of the middle and inferior turbinates.

Peele (1957) discussed that “normal” SS are quite rare and extension of the sinuses are so commonplace that they must be viewed as representative of the anatomy of this region [11]. He documented that the SS could occasionally open into a posterior ethmoid cell (PEC); also other rare possibilities were listed, all of these being unilateral [11]. Peele (1957) also mentioned the ethmoidal recess of the SS which, in the author’s experience, may invade the posterior ethmoid and “is most likely to occur at the postero-lateral-inferior angle of the ethmoidal labyrinth” and “may extend [...] superiorly as far forward as the bulla, thus coming into rather extensive relationship with the orbit, antrum, or supraorbital extension of the frontal sinus [...]” [11]. Peele (1957) located the ethmoidal recess of the SS in front of the sphenopalatine pillar. Previously, Van Alyea (1941) described such an ethmoidal

recess of the SS, but did not term it, and indicated that it passes over the sphenopalatine elevation [above the sphenopalatine or pterygopalatine ganglion (PPG)] to invade the ethmoid field and to occasionally reach the orbital wall [2]. The SS recesses directed towards the pterygopalatine angle of the maxillary sinus (MS) were termed maxillary recesses of the SS [12–14]. Although different studies indicate various anatomic possibilities of SS pneumatization [12–16], a consistent ethmoidal pneumatization determining large unique sphenothmoidal sinuses (SESs) was not described, in our knowledge.

Several possible mechanisms could be reasonably speculated for the morphogenesis of such a SES. Either a mechanism of fusion would unite the primary and the secondary pneumatizations of the developing SS, or the postnatal *concha sphenoidalis*, which separates the posterior ethmoid and the SS could be resorbed and, subsequently, the most posterior ethmoid air cell would be incorporated to the SS. Thirdly, if the SS develops as an extension of the postero-superior portion of the sphenothmoidal recess [17], which excavates the *concha sphenoidalis* [18], the SES could be related with an abnormal anterior length of the sphenoid body which penetrates anteriorly the nasal fossa roof and lateral wall and shortens sagittally a morphologically normal ethmoid.

Aim

We therefore aimed at documenting retrospectively a group of human adult skulls scanned in cone-beam computed tomography (CBCT) to test the occurrence of such SES and whether, or not, they relate to a sagittally shortened ethmoid.

☐ Patients, Materials and Methods

A retrospective CBCT study of the archived files of 36 adult patients (1:1 gender ratio) was performed. The subjects were scanned using an iCat (Imaging Sciences International) CBCT machine with the settings described in previous studies [12, 19]. The Digital Imaging and Communications in Medicine (DICOM) files were documented with the Planmeca Romexis Viewer 3.5.0.R software. We evaluated the sinonasal anatomy on planar slices and on three-dimensional (3D) volume renderizations. Relevant anatomical features were exported as image files. The patients have given written informed consent for the use of the anonymized CBCT data for research purpose.

To test the hypothesis, we measured the *nasion-to-concha sphenoidalis* (N–CS) sagittal distances.

Statistical analysis was performed using Statistical Package for the Social Sciences (SPSS) for Mac. We used descriptive statistics (mean, standard deviation), Analysis of Variance (ANOVA), and regression analysis. A *p*-value less than 0.05 was considered statistically significant.

☐ Results

A total number of 36 cases were included in the analysis, the gender ratio being 1:1.

The average right N–CS sagittal distance was 43.27 mm, almost equal in male (43.4 mm) and female (43.14 mm) subjects. The difference between genders is not statistically

significant (ANOVA test, $F=0.095$, $p=0.76$). The distribution of the values on the right side in each gender is presented in Figure 1.

The average left N–CS sagittal distance was 43.97 mm, slightly larger for males (44.62 mm) than females (43.3 mm). The difference between genders is not statistically significant (ANOVA test, $F=0.978$, $p=0.330$), but larger compared to the right N–CS sagittal distance. The distribution of the values on the left side in each gender is presented in Figure 2.

In Figure 3 is shown the distribution of the cases based on left/right *nasion–concha sphenoidalis* sagittal distance. The regression equation best fitting the results is cubic (having an R^2 value of 0.471); in women, the differences between left and right seem to be smaller at average values but tend to be more dispersed at higher values, while for males the dispersion is more homogenous.

Right-sided SES (Figure 4) was encountered in three cases, the average N–CS sagittal distance in subjects with pneumatization being 38.56 mm, significantly lower than the value obtained in subjects without right-sided pneumatization (43.7 mm). The difference was statistically significant, at a $p<0.001$ (ANOVA test, $F=16.7$).

Left-sided SES (Figure 5) was encountered in five cases, the average N–CS sagittal distance in subjects with pneumatization being 39.02 mm, significantly lower than the value obtained in subjects without right-sided pneumatization (44.78 mm). The difference was statistically significant, at a $p=0.001$ (ANOVA test, $F=12.28$).

In 6/36 cases, we found pneumatic cavities located within the sphenoid body and extended anteriorly in the posterior ethmoidal region, above the posterior ends (tails) of the MTs. We considered these cavities as SES. In 2/6 SES cases they were bilateral, in the other 4/6 cases they were unilateral (Figure 6), one on the right side, the other on the left side.

In one male patient (Figure 7) with bilateral evidence of such SES, they were equally sized and bi-cameral – each one had an anterior ethmoidal and, respectively, a posterior sphenoidal chamber, these being separated by incomplete septa inserted on the sphenopalatine (pterygopalatine) elevation of Van Alyea. The ostium of each SES was located medially to the ST and opened into the sphenothmoidal recess. Additional evidence was gathered in this case about the MS. The respective sinuses presented each two recesses of their posterior walls, a posterior superior one, directed towards the SES, and a posterior inferior one, directed towards the pterygoid process, thus a pterygoid recess. Between the respective two recesses was the PPG fossa. Each pterygoid recess was attaching the MT. The superior turbinates (STs) were bilaterally present but they were differently attached: the left ST had anterior ethmoidal and posterior SES insertions, while the right ST had anterior ethmoidal and posterior maxillary insertions, this later on the medial wall of that MS.

In a female patient, we also got bilateral evidence of SES. Similar insertions of the STs were found, such as in the previously detailed case. None of the other cases we studied presented a maxillary insertion of the ST. In this case, we noted the perforated right MT, which allowed the middle nasal meatus communication with the parasseptal area (Figure 8).

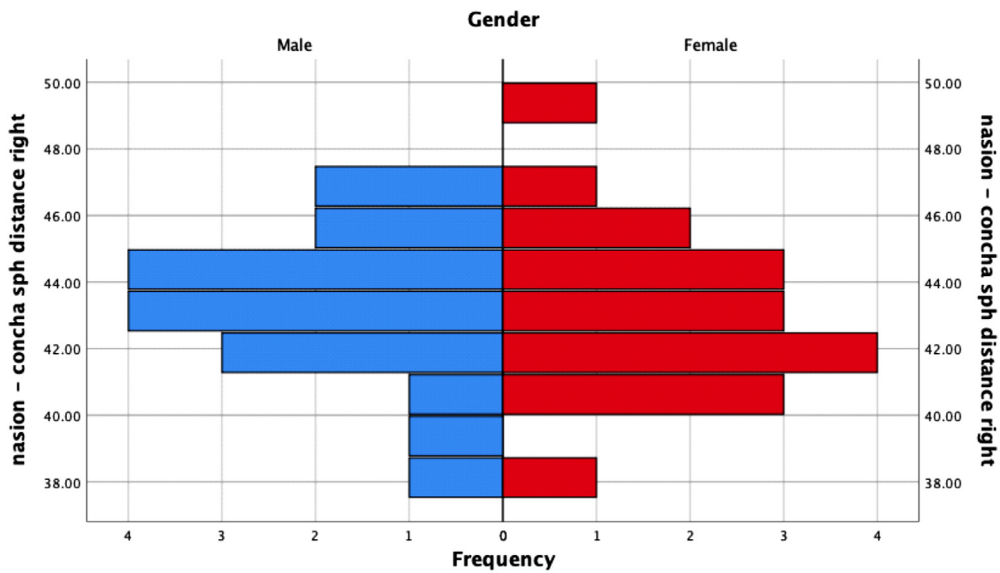


Figure 1 – Right nasion-concha sphenoidal distance, distribution depending on the gender.

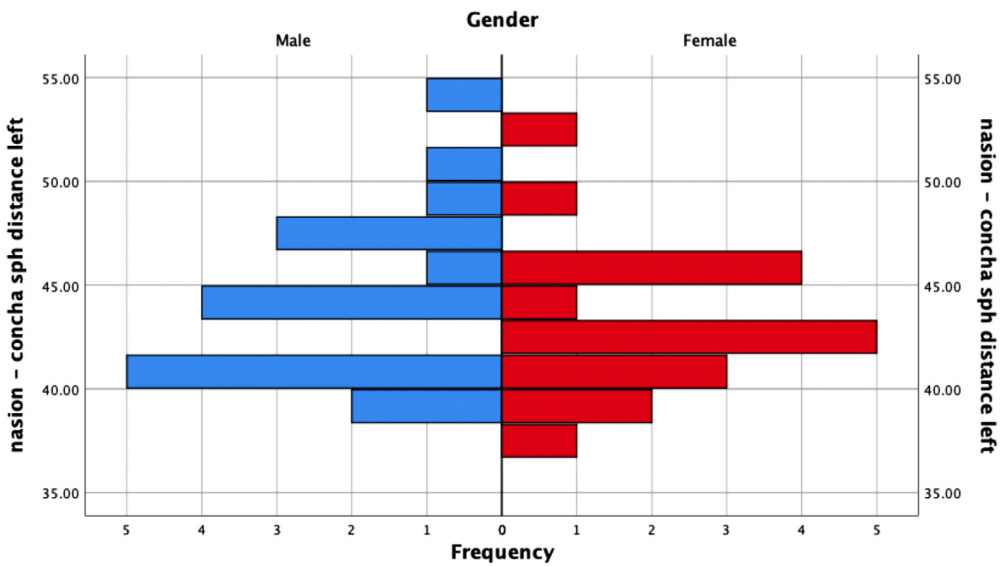


Figure 2 – Left nasion-concha sphenoidal distance distribution depending on the gender.

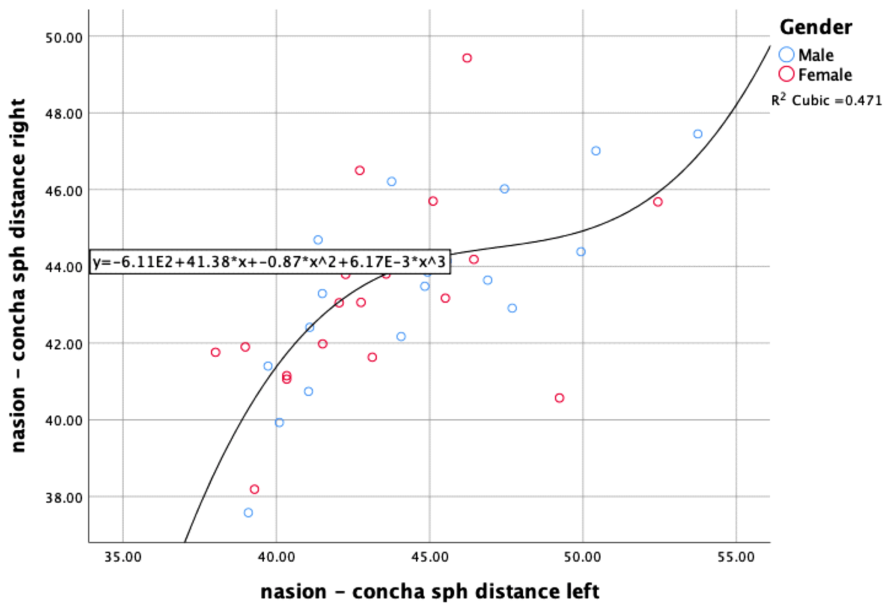


Figure 3 – Scatter dot left/right nasion-concha sphenoidal distance, and regression analysis.

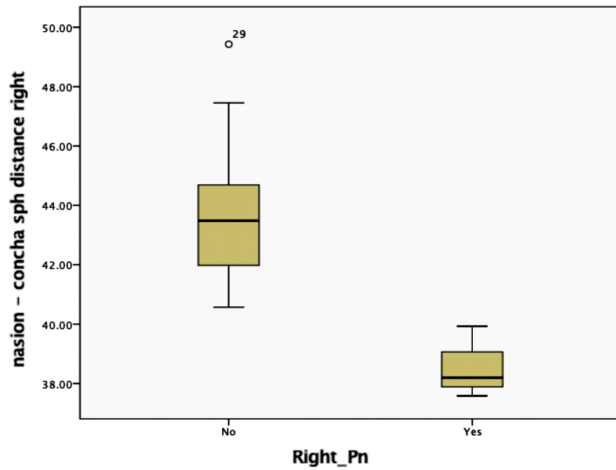


Figure 4 – Right nasion–concha sphenoidalis sagittal distance in subjects with/without pneumatization (Pn).

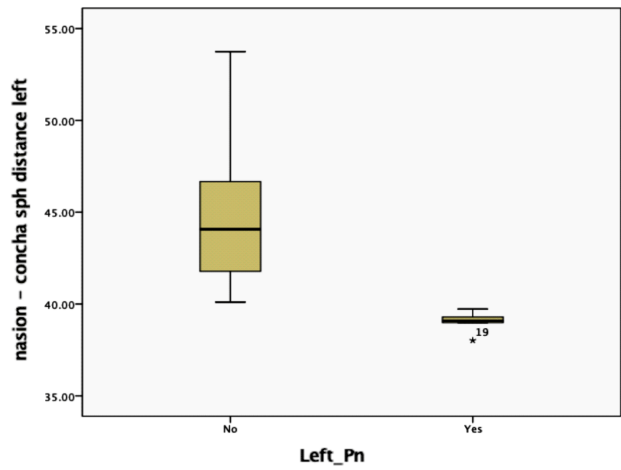


Figure 5 – Left nasion–concha sphenoidalis sagittal distance in subjects with/without pneumatization (Pn).

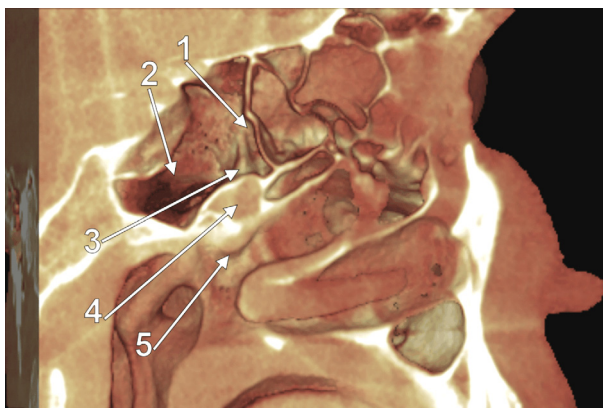


Figure 6 – Three-dimensional volume rendering of the left lateral nasal wall. 1: Anterior ethmoidal chamber of the SES; 2: Posterior sphenoidal chamber of the SES; 3: Van Alyea’s elevation; 4: Pterygopalatine fossa; 5: Tail of the middle nasal turbinate. SES: Sphenoethmoidal sinus.

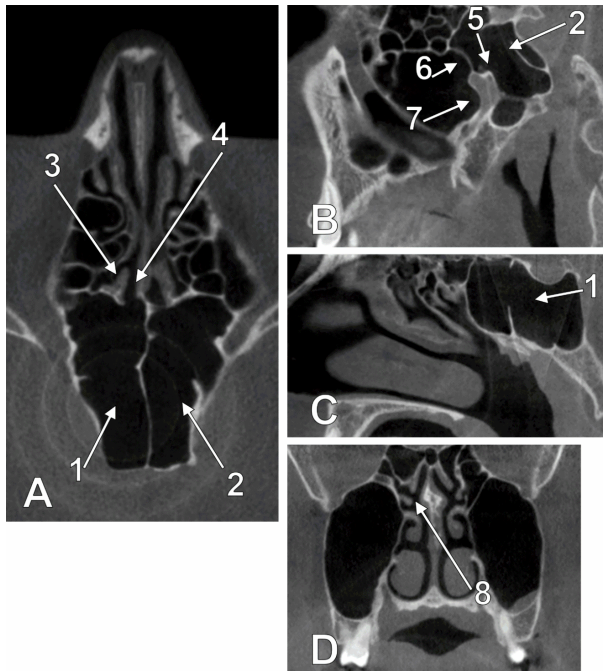


Figure 7 – Bi-dimensional slices of bilateral SESs (A – axial slice; B – left sagittal slice; C – right sagittal slice) and MSs (D – coronal slice). 1: Right SES; 2: Left SES; 3: Right superior turbinate; 4: Sphenoethmoidal recess; 5: Van Alyea’s elevation; 6: Posterior superior recess of the posterior wall of the left MS; 7: Pterygoid recess of the posterior wall of the left MS; 8: Right superior nasal turbinate inserted onto the MS wall. SES: Sphenoethmoidal sinus; MS: Maxillary sinus.

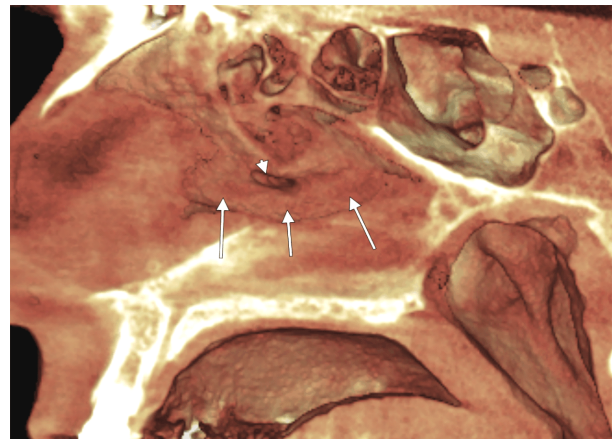


Figure 8 – Three-dimensional volume rendering of the right lateral nasal wall. The middle nasal turbinate (arrows) has a perforation (arrowhead) in its middle third.

Discussions

The thorough understanding of sinus anatomy is critical to adequately perform functional endoscopic sinus surgery (FESS), and the concept of paranasal surgical box forms the framework of FESS [20]. A functional classification of the paranasal sinuses relies on their drainage pathways [20]. The posterior functional complex includes the posterior ethmoid cells and the SS [20]. Therefore, a SES variant modifies the posterior functional cavity into a morphological one.

The greater the degree of SS pneumatization is, the easier it is to identify the landmarks within the sinus during transsphenoidal approaches [21].

The SES modifies the landmarks provided by the nasal turbinates and the anatomy of the sphenoidal recess. According to Harvey *et al.* (2010), quoted in Dalgorf & Harvey (2013), the ostium of the SS is behind the ST within the sphenoidal recess, at the level of the MS roof [20, 22]. The SES pneumatization we documented here brought that ostium above and not behind the ST. Thus, an unidentified SES and a routine use of the ST landmark could lead to undesired endoscopic corridors during FESS.

Moreover, to our knowledge, the insertion of the ST on the medial wall of the MS was not reported previously, although different other morphological possibilities of the nasal turbinates were documented [23–29]. Surgeons who identify the ST are commonly convinced that lateral to it are ethmoidal cells. Therefore, in the situation of a ST with maxillary insertion, such as in a SES variant, the risk of opening the MS instead of the ethmoid sinus is great. We checked the cases with unilateral SES, and we found that none had such maxillary insertions of the STs. It is therefore possible for the sphenoidal pneumatizations not to be a determinant, or result, of a maxillary attachment of the ST. Further studies should test whether, or not, there is a correlation between the height of the orbit, that of the MS, and that of the ethmoidal labyrinth.

We found unilateral perforation of the middle nasal turbinate which allowed the middle nasal meatus to communicate directly with the paraseptal space. We could not find any previous reports of such turbinate perforation.

Different anatomic possibilities for the MS pneumatization are actually known and include the postero-superior extension towards the SS, which was termed sphenoidal recess of the MS [13]. In a SES case, such a MS recess may become a sphenoidal one, as we found here. However, we could not find any previous description of a posterior pterygoid recess of the MS located inferior to the PPG. This anatomic possibility should be checked if the pterygopalatine corridor is intended during endoscopic approaches.

☐ Conclusions

Márquez *et al.* (2008) pointed that “*the sole guide to the morphological identity of a sinus is provided not by the bone or bones it may ultimately pneumatize, but by the bone or bones that circumscribe its ostium, or point of origin*” [1]. The SES drains through an ostium on its anterior wall, as the SS does, but it invades the situs of the posterior ethmoid and it shortens sagittally the nasal roof and the lateral nasal wall. Therefore, the sagittal pneumatization of the SS should not be graded only in an anterior-to-posterior direction by referring it to the *sella turcica*, but also in a posterior-to-anterior direction, as SS, or SES.

☐ Conflict of interests

All authors declare that there is no conflict of interests.

References

- [1] Márquez S, Tessema B, Clement PA, Schaefer SD. Development of the ethmoid sinus and extramural migration: the anatomical basis of this paranasal sinus. *Anat Rec (Hoboken)*, 2008, 291(11):1535–1553. <https://doi.org/10.1002/ar.20775> PMID: 18951481
- [2] Van Aleya OE. Sphenoid sinus: anatomic study, with consideration of the clinical significance of the structural characteristics of the sphenoid sinus. *Arch Otolaryngol*, 1941, 34(2):225–253. <https://doi.org/10.1001/archotol.1941.00660040251002>
- [3] Orhan M, Govsa F, Saylam C. A quite rare condition: absence of sphenoidal sinuses. *Surg Radiol Anat*, 2010, 32(6):551–553. <https://doi.org/10.1007/s00276-010-0623-7> PMID: 20082077
- [4] Weiglein A, Anderhuber W, Wolf G. Radiologic anatomy of the paranasal sinuses in the child. *Surg Radiol Anat*, 1992, 14(4):335–339. <https://doi.org/10.1007/BF01794761> PMID: 1290149
- [5] Zada G, Agarwalla PK, Mukundan S Jr, Dunn I, Golby AJ, Laws ER Jr. The neurosurgical anatomy of the sphenoid sinus and sellar floor in endoscopic transsphenoidal surgery. *J Neurosurg*, 2011, 114(5):1319–1330. <https://doi.org/10.3171/2010.11.JNS10768> PMID: 21235317 PMID: PMC4131853
- [6] Săndulescu M, Rusu MC, Ciobanu IC, Ilie A, Jianu AM. More actors, different play: sphenoidal cell intimately related to the maxillary nerve canal and cavernous sinus apex. *Rom J Morphol Embryol*, 2011, 52(3):931–935. PMID: 21892542
- [7] Kayalioglu G, Erturk M, Varol T. Variations in sphenoid sinus anatomy with special emphasis on pneumatization and endoscopic anatomic distances. *Neurosciences (Riyadh)*, 2005, 10(1):79–84. PMID: 22473192
- [8] Idowu OE, Balogun BO, Okoli CA. Dimensions, septation, and pattern of pneumatization of the sphenoidal sinus. *Folia Morphol (Warsz)*, 2009, 68(4):228–232. PMID: 19950072
- [9] Keskin G, Ustündag E, Ciftçi E. Agenesis of sphenoid sinuses. *Surg Radiol Anat*, 2002, 24(5):324–326. <https://doi.org/10.1007/s00276-002-0028-3> PMID: 12497225
- [10] Vasvári G, Reisch R, Patonay L. Surgical anatomy of the cribriform plate and adjacent areas. *Minim Invasive Neurosurg*, 2005, 48(1):25–33. <https://doi.org/10.1055/s-2004-830180> PMID: 15747213
- [11] Peele JC. Unusual anatomical variations of the sphenoid sinuses. *Laryngoscope*, 1957, 67(3):208–237. <https://doi.org/10.1288/00005537-195703000-00004> PMID: 13417674
- [12] Rusu MC, Didilescu AC, Jianu AM, Păduraru D. 3D CBCT anatomy of the pterygopalatine fossa. *Surg Radiol Anat*, 2013, 35(2):143–159. <https://doi.org/10.1007/s00276-012-1009-9> PMID: 22918475
- [13] Craiu C, Rusu MC, Hostiuc S, Săndulescu M, Derjac-Aramă AI. Anatomic variation in the pterygopalatine angle of the maxillary sinus and the maxillary bulla. *Anat Sci Int*, 2017, 92(1):98–106. <https://doi.org/10.1007/s12565-015-0320-z> PMID: 26663153
- [14] Ciobanu IC, Motoc A, Jianu AM, Cergan R, Banu MA, Rusu MC. The maxillary recess of the sphenoid sinus. *Rom J Morphol Embryol*, 2009, 50(3):487–489. PMID: 19690779
- [15] Elwany S, Elsaied I, Thabet H. Endoscopic anatomy of the sphenoid sinus. *J Laryngol Otol*, 1999, 113(2):122–126. <https://doi.org/10.1017/s0022215100143361> PMID: 10396560
- [16] Andrei F, Motoc AG, Jianu AM, Rusu MC, Loreto C. The pneumatization patterns of the roof of the parapharyngeal space in CBCT. *Germs*, 2012, 2(4):142–147. <https://doi.org/10.11599/germs.2012.1026> PMID: 24432276 PMID: PMC3882848
- [17] Davis WB. LV. Anatomy of the nasal accessory sinuses in infancy and childhood. *Ann Otol Rhinol Laryngol*, 1918, 27(3):940–967. <https://doi.org/10.1177/000348941802700308>
- [18] Sivasli E, Sirikçi A, Bayazıt YA, Gümüşburun E, Erbagci H, Bayram M, Kanlykama M. Anatomic variations of the paranasal sinus area in pediatric patients with chronic sinusitis. *Surg Radiol Anat*, 2003, 24(6):400–405. <https://doi.org/10.1007/s00276-002-0074-x> PMID: 12652368
- [19] Rusu MC, Sava CJ, Ilie AC, Săndulescu M, Dincă D. *Agger nasi cells versus lacrimal cells and uncinata bullae in cone-beam computed tomography*. *Ear Nose Throat J*, 2019, 98(6):334–339. <https://doi.org/10.1177/0145561319840836> PMID: 31012345
- [20] Dalgorf DM, Harvey RJ. Chapter 1: Sinonasal anatomy and function. *Am J Rhinol Allergy*, 2013, 27(3 Suppl):S3–S6. <https://doi.org/10.2500/ajra.2013.27.3888> PMID: 23711029

- [21] Wang Q, Lan Q, Lu XJ. Extended endoscopic endonasal trans-sphenoidal approach to the suprasellar region: anatomic study and clinical considerations. *J Clin Neurosci*, 2010, 17(3):342–346. <https://doi.org/10.1016/j.jocn.2009.05.032> PMID: 20074954
- [22] Harvey RJ, Shelton W, Timperley D, Debnath NI, Byrd K, Buchmann L, Gallagher RM, Orlandi RR, Sacks R, Schlosser RJ. Using fixed anatomical landmarks in endoscopic skull base surgery. *Am J Rhinol Allergy*, 2010, 24(4):301–305. <https://doi.org/10.2500/ajra.2010.24.3473> PMID: 20819470
- [23] Rusu MC, Săndulescu M, Sava CJ, Dincă D. Bifid and secondary superior nasal turbinates. *Folia Morphol (Warsz)*, 2019, 78(1):199–203. <https://doi.org/10.5603/FM.a2018.0047> PMID: 29802719
- [24] Sava CJ, Rusu MC, Săndulescu M, Dincă D. Vertical and sagittal combinations of *concha bullosa* media and paradoxical middle turbinate. *Surg Radiol Anat*, 2018, 40(7):847–853. <https://doi.org/10.1007/s00276-018-1998-0> PMID: 29502247
- [25] Măru N, Rusu MC, Săndulescu M. Variant anatomy of nasal turbinates: supreme, superior and middle *conchae bullosae*, paradoxical superior and inferior turbinates, and middle accessory turbinate. *Rom J Morphol Embryol*, 2015, 56(3): 1223–1226. PMID: 26662164
- [26] Rusu MC, Măru N, Sava CJ, Motoc A, Săndulescu M, Dincă D. The sagittal grooves of the middle nasal turbinate determine paradoxical curvatures and bifidities. *Niger J Clin Pract*, 2020, 23(4):464–469. https://doi.org/10.4103/njcp.njcp_63_19 PMID: 32246651
- [27] San T, Erdoğan B, Taşel B. Triple-divided *concha bullosa*: a new anatomic variation. *Case Rep Otolaryngol*, 2013, 2013:342615. <https://doi.org/10.1155/2013/342615> PMID: 24222880 PMCID: PMC3810058
- [28] San T, Gurkan E, Erdogan B. An unusual anatomical variation of the superior turbinate: a case report. *J Med Case Rep*, 2014, 8:182. <https://doi.org/10.1186/1752-1947-8-182> PMID: 24912569 PMCID: PMC4090649
- [29] Yanagisawa E, Mirante JP, Christmas DA. Vertical insertion of the middle turbinate: a sign of the presence of a well-developed *agger nasi* cell. *Ear Nose Throat J*, 2002, 81(12): 818–819. PMID: 12516371

Corresponding author

Mugurel Constantin Rusu, Professor, MD, PhD, Dr. Hab., Division of Anatomy, Faculty of Dental Medicine, Carol Davila University of Medicine and Pharmacy, 8 Eroilor Sanitari Avenue, Sector 5, 050474 Bucharest, Romania; Phone +40722–363 705, e-mail: mugurel.rusu@umfcd.ro

Received: January 30, 2020

Accepted: April 22, 2020